

Low-pressure nano-silica injection on cement for crack-healing and water transport

R. Maddalena & A. Hamilton

Department of Civil and Environmental Engineering, University of Strathclyde, Glasgow - UK

A. K. Mali

Department of Civil Engineering, IIT Bombay, Mumbai - India

ABSTRACT: Durability of building materials is related to the presence of cracks since they provide a fast pathway to the transport of liquid and gasses through the structure. Restoration and preservation of historical buildings has been investigated through the application of novel cementitious materials using nanoparticles such as nano-silica and silica fume. The small particle size range and the high reactivity of nanoparticles allow them to interact with calcium sources naturally present in construction materials and forming binding and strengthening compounds such as calcium silicate hydrates. Nanoparticles act as a crack-filler agent, reducing the porosity and increasing the durability of the existing material. Injection of nano-silica was carried out at a low water pressure in hydrated cement paste. This novel technique can tailor mechanical and hydraulic properties of existing building materials simply and non-destructively.

1 INTRODUCTION

Most of the built environment is made using concrete and many historical buildings constructed in 1950's and later suffer from crack formation, alkali-silica reaction and water penetration. Cracking in concrete and mortar is an inevitable phenomenon of ageing and erosion. Thus, material characteristics such as porosity, permeability, strength and density are altered during ageing.

Hardened concrete and cement contain two important mineral phases: calcium hydroxide (portlandite) and calcium silicate hydrates (C-S-H), the former has a defined crystalline structure, the latter is semi-crystalline (Pellenq et al. 2008). C-S-H is the phase responsible for strength development in concrete and can be up to 70% of total volume of hardened concrete (Chen et al. 2004). In cementitious materials, C-S-H is produced by hydration of alite and belite (tricalcium silicate and dicalcium silicate respectively). Pozzolanic material such as fly ash, slag, rice husk ash and silica fume can be added which can increase the amount of C-S-H produced and thus improve mechanical performance (Sha 2002; Sanchez & Sobolev 2010).

The formation of cracks and increased porosity from leaching in concrete and cement paste presents an easy pathway for the ingress of moisture. Gaps and cracks can be reduced by the treating with nanoparticle consolidants. In the work presented here, the injected silica reacts with portlandite naturally present in hydrated cement paste to form new cementi-

tious material and reduce the porosity of the system. The result is increased durability and life-time (Cardenas & Struble 2006; Hou et al. 2014; Sánchez et al. 2014; Hou et al. 2015).

Research on partial replacement of cement clinker with nano-silica (Li et al. 2004) found that increasing the quantity of nano-silica replacing cement from 3% to 5% vol. increased the mechanical strength of mortar by acceleration of the hydration reaction and the filler effect of nano-particles. They also observed a dense and compact texture of hydrated paste and an absence of portlandite crystals, suggesting that most of the calcium hydroxide had reacted with the nano-silica added. This result was confirmed by Tao Ji and Qing et al. (Ji 2005; Qing et al. 2007). Nano-silica addition to cement paste has been shown to increase C-S-H formation and accelerate dissolution of unreacted alite (C_3S) due to the high reactivity of small particles (Björnström et al. 2004). Tao Ji observed that the average water penetration depth of concrete made with fly ash and cement was 14.6 cm under low applied pressure whereas concrete mixed with nano-silica was 8.1 cm under high pressure, confirming the improvement in water penetration resistance when nano-silica is added (Ji 2005). He concluded that the pozzolanic reaction of fly ash in presence of nano-silica was accelerated compared to ordinary Portland cement (OPC). Qing et al. reported little acceleration in setting time of fresh paste with increasing nano-silica content but some enhancement of compressive strength. Pozzolanic reactivity of nano-silica is high-

er than the silica fume, due to the smaller particle size and higher specific surface area (Qing et al. 2007). Varying the nano-silica content (3%, 6%, 9%, and 12% wt.) in mortar produced an increase in strength with decrease in calcium hydroxide content. The heat of hydration was also increased by addition of nano-silica from the rapid hydration of silicates (Jo et al. 2007).

The aim of this work was to find a non-destructive and easily applied conservation treatment for cement and concrete. In this study the effect of nano-silica and silica fume injection in hardened cement paste was investigated by quantitative analysis of hydration products (C-S-H and portlandite) present.

2 MATERIALS AND METHODS

2.1 Materials

The experiments were carried out on pure hardened cement paste, using ordinary Portland cement CEM I (Table 1) and deionized water. Nano-silica suspension LUDOX T-50 and silica fume ELKEM micro-silica were used (Table 2).

Table 1. Characteristic of CEM I Portland cement.

Components	CEM I %
Clinker	100
Gypsum added	7
Chemical composition (>0.2%)	
SiO ₂	23.7
Al ₂ O ₃	2.8
Fe ₂ O ₃	2.3
CaO	67.3
MgO	0.7
SO ₃	1.9
K ₂ O/Na ₂ O	0.2
Density (g/cm ³)	3.2
Specific area (m ² /g)	0.31
Compressive strength, 28 days (MPa)	60

Table 2. Characteristics of nano-silica (NS) and silica fume (SF).

Components	NS	SF
	%	%
State	Acqueous suspension	Densified
Chemical composition (>0.2%)		
SiO ₂	50	99.9
Water	50	-
Particle size range (nm)	5-20	150-1000
Density (g/cm ³)	1.4	1.56
Specific area (m ² /g)	160	21.5

2.2 Sample preparation

Cement samples were prepared mixing Portland cement and deionized water at a water to cement (w/c) ratio of 0.41. The mixing of cement and water was

made in a rotary mixer according to BS EN 196-1:2005. Cement paste was cast into plastic moulds (35mm Ø and 4mm thickness, disc-shaped) and cured under controlled conditions (relative humidity of 98 ± 2% and temperature of 21 ± 2 °C). After 28 days, cement discs were oven-dried at 60 °C for ca. 100 hours, until the change in weight was negligible. Drying temperature of 60 °C was chosen because it does not affect the pore-structure and mineralogy of the cement paste (Gallé 2001; Korpa & Trettin 2006; Zhang & Scherer 2011).

2.3 Experimental setup

Nano-silica injection was carried out by varying three parameters: injection period, percentage of nano-silica injected and silica particle size (NS or SF) with a constant applied pressure head. Silica solutions were prepared using nano-silica stock suspension or solid silica fume, mixed with deionized water. In order to investigate how the penetration depth in the disc varies with nano-silica content, three different percentages (10%, 15% and 20% wt.) were used, for a total injection time of 14 days. The effect of injection time was determined by keeping cement discs under injection for 7, 14 and 28 days with 10% wt. nano-silica content. To compare the reactivity and effect of particle size on penetration depth, samples were injected with 10% and 20% of silica fume for the period of 14 days (Table 3).

The cement disc was fixed in place at the bottom of a PVC pipe of 2 m length and 40 mm internal diameter (Figure 1). The pipe was then held vertically by clamping it with stands. The solution of nano-silica at a given concentration was slowly poured into the pipe from the top, in order to minimize the density gradient. The length of pipe used gives a constant hydrostatic pressure of 20 kPa at the bottom of the pipe, where the OPC specimen is placed. After filling the pipe, a plastic cap was placed at the top of the pipe to avoid evaporation of the solution. At the end of the injection period the disc was removed and oven-dried at 60 °C for ca. 100 hours. The sample weight was recorded before and after the injection to quantify the amount of silica in the pores.

Table 3. Experimental data and sample details.

Sample	Injected silica NS or SF	Silica content %	Injection period days
S10-14	NS	10	14
S15-14	NS	15	14
S20-14	NS	20	14
S10-7	NS	10	7
S10-28	NS	10	28
SF10-14	SF	10	14
SF20-14	SF	20	14

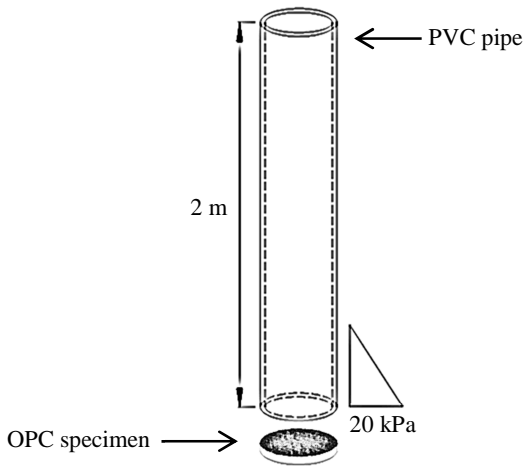


Figure 1. Experimental set-up model.

2.4 Microstructural analysis

The capability of injected silica to react with calcium hydroxide (CH) present in the hydrated cement paste to form additional calcium silicate hydrates (C-S-H) was determined by the quantity of calcium hydroxide and calcium silicate hydrates in the treated hydrated cement paste compared with the control sample by thermogravimetric analysis (TGA). An average of 20 mg was sampled from the cross section of the disc and powdered. Thermal analyses were conducted at a heating rate of $10\text{ }^{\circ}\text{C min}^{-1}$ from $25\text{ }^{\circ}\text{C}$ to $1000\text{ }^{\circ}\text{C}$ under nitrogen gas flow, using a Netzsch simultaneous analyzer.

Mineralogical composition of silica injected specimens was analyzed by powder X-ray diffraction (XRD) technique using a Bruker D8 Advance diffractometer, from 5° to $60^{\circ}2\theta$, at a rate of $1^{\circ}/\text{min}$ and a step size of $0.02^{\circ}2\theta$. In order to estimate silica entrainment through the pores, sample disc weight was recorded before and after silica injection, at $60\text{ }^{\circ}\text{C}$ oven-dried conditions. Open porosity (ψ) was estimated by measuring the total water amount in each sample after oven-drying at $60\text{ }^{\circ}\text{C}$ and overnight saturation in a vacuum chamber. Open porosity was calculated as follows (Equation 1):

$$\psi = \frac{m_s - m_d}{V \cdot \rho} \quad (1)$$

where ψ is the open porosity, m_s is the sample water saturated mass (kg), m_d is the sample dried mass (kg), V is the volume of the sample (m^3) and ρ is the density of the water at $20\text{ }^{\circ}\text{C}$ (kg/m^3).

Microstructural analysis of samples was characterized using field emission Scanning Electron Microscopy (SEM, Hitachi SU6600) and Energy Dispersive Spectroscopy (EDS, Oxford INCA-7260) with an accelerating voltage of $10 - 15\text{ kV}$. All samples were resin impregnated, polished and gold coated.

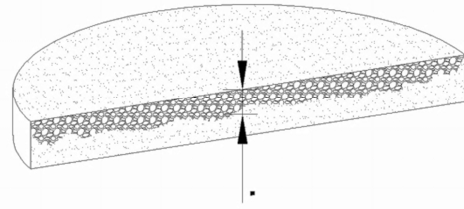


Figure 2. Model of silica penetration depth on OPC sample after injection.

3 RESULTS AND DISCUSSION

3.1 Weight change and porosity measurements

Mass measurements show that after 14 days of injection of nano-silica the mass increase is directly proportional to the silica concentration in the solution (Figure 3). At a given nano-silica content in the pipe of 10% wt., the sample mass shows an exponential trend reaching 2.0 wt% mass gains at 28 days (Figure 4). A comparison between nano-silica and silica fume show the effect of particle size on the injection: doubling the concentration of nano-silica results in an increase of weight of ca. +1%, whereas doubling the silica fume content results in an increase of weight of ca. +0.1%. This is due to the low particle size range of nano-silica ($5 - 20\text{ nm}$), able to penetrate into smaller pores. Open porosity (ψ) measurements show that an increase in nano-silica content in the solution produces a significant decrease in porosity of ca. 30%, from the initial value (sample OPC, $\psi = 0.30$) to the highest concentration at 20% wt. (sample S20-14, $\psi = 0.20$), as shown in Figure 5. Injection of silica-fume, on the other hand does not produce a significant porosity reduction (Qing et al. 2007). Injection time at the lowest nano-silica content (10% wt.) shows a reduction in porosity of ca. 20%, from the initial value (sample OPC, $\psi = 0.30$) to the longest injection time (sample S10-28, $\psi = 0.24$) as shown in Figure 6.

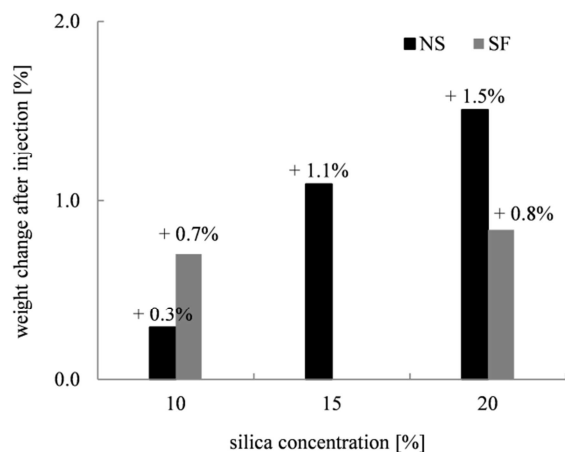


Figure 3. Influence of nano-silica concentration on weight increase after injection for 14 days.

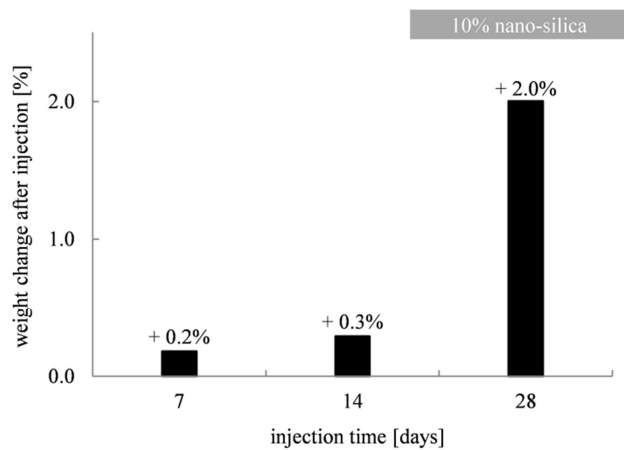


Figure 4. Influence of injection time on weight increase at 10% nano-silica concentration.

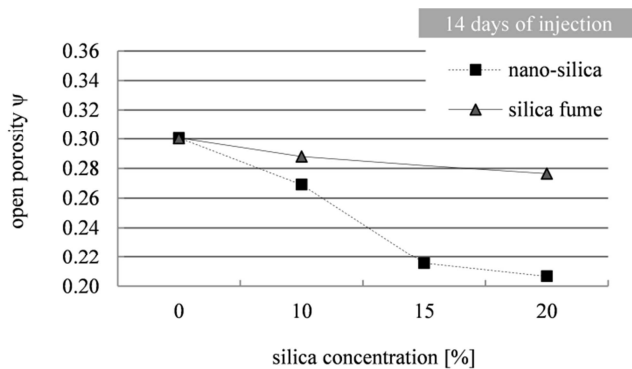


Figure 5. Influence of silica concentration on porosity after injection for 14 days.

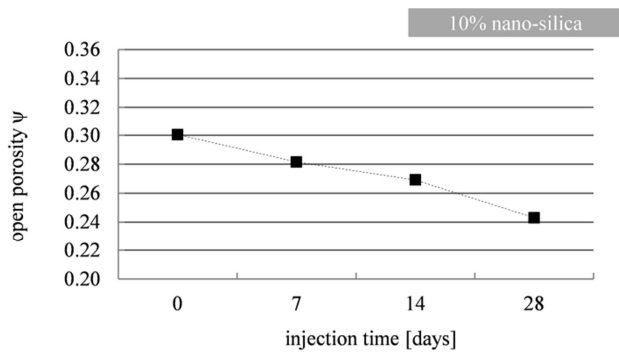


Figure 6. Influence of injection time on weight increase at 10% nano-silica concentration.

3.2 Thermal analysis

Figure 7 shows the thermogravimetric (TG) curves for selected samples. The weight loss is in % with respect to temperature (25 – 1000 °C). All samples show TG curves typical of Portland cement, having maximum weight loss from room temperature to 200 °C. The weight loss in the range 80 – 150 °C is attributed to C-S-H gel, calcium aluminate silicate hydrate (C-A-S-H) gel, ettringite and other minor compounds (Sha et al. 1999; Sha & Pereira 2001;

Klimesch et al. 2002). The thermogravimetric step in the range 400 – 460 °C is assigned to the portlandite dehydration (CH). Weight loss over the range 530 – 660 °C may be attributed to the loss of CO₂ from any calcium carbonate present. All samples show a slight weight loss in the range 700 – 780 °C due to the dehydroxylation of silanol Si-O-H groups (Garbev et al. 2008; Shaw et al. 2000). Table 4 shows the TG values in the C-S-H range and portlandite range.

Figure 7. TG curves of selected samples.

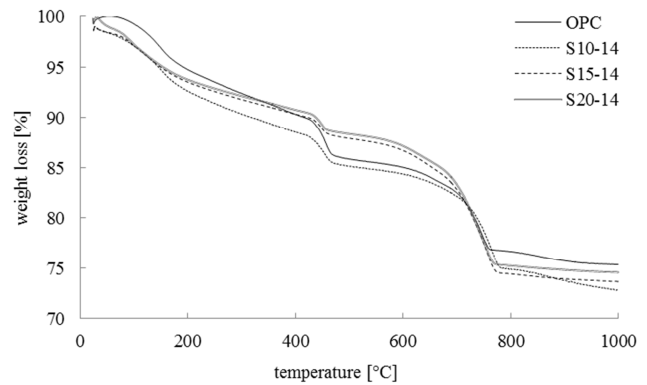


Table 4. Summary of the TG analysis results for each sample.

Sample	C-S-H/C-A-S-H	CH
	80 - 150 °C	400 - 460 °C
	%	%
OPC	2.89	3.35
S10-14	3.02	2.68
S15-14	3.04	1.96
S20-14	3.09	2.03
S10-7	2.80	2.70
S10-28	2.81	2.15
SF10-14	2.8	2.25
SF20-14	3.01	2.09

Figure 8 shows the CH content reduction due to the reaction of CH with nano-silica and additional formation of C-S-H can be observed when the nano-silica concentration is increased. This reduction of about 40% of the initial content is higher compared to the values found in literature (Cardenas & Struble 2006; Sánchez et al. 2014). Figure 10 shows the consumption of CH with time (injection period) and slight increase of C-S-H content. There is no evidence of CH reduction when the nano-silica content is increased beyond 15 wt% in the injecting solution. Figure 9 suggests that the ideal injection period is 28 days, producing a CH reduction of ca. 1.2%. Thermal data of nano-silica and silica fume for 14 days injection time show that both materials offer a comparable CH reduction at the highest concentration (20% wt.).

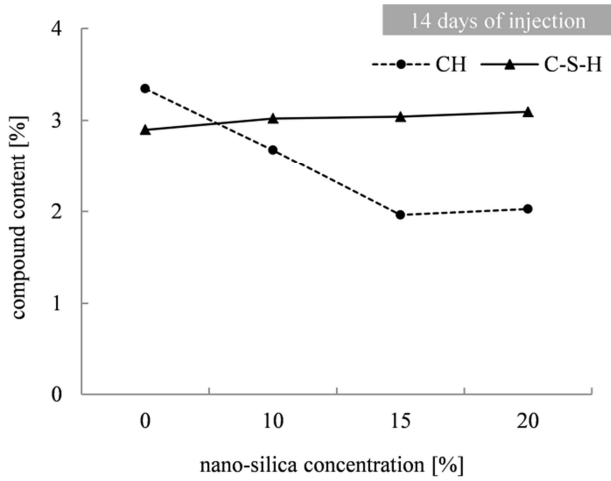


Figure 8. TG data. Effect of nano-silica percentage on compounds content.

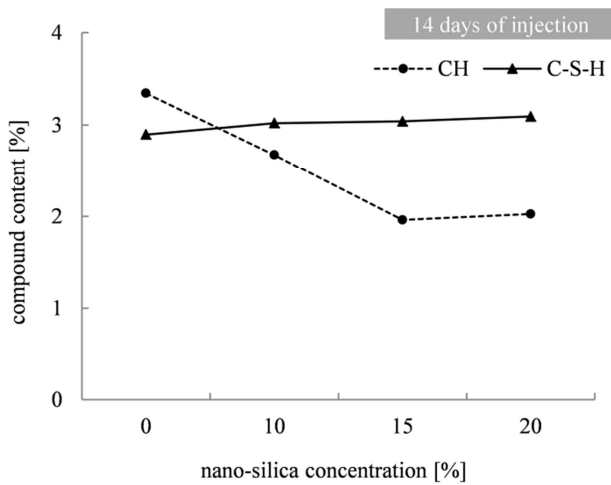


Figure 9. TG data. Effect of injection time on compounds content.

3.3 XRD analysis

XRD analysis of the injected samples (Figure 10) show a progressive decrease in intensity of portlandite peaks. Calcium aluminate phases (C_3A , peak at ca. $11.5^\circ 2\theta$), present in the original clinker reacted with nano-silica forming additional C-S-H/C-A-S-H (calcium aluminate silicate hydrate), observed at ca. $15.5^\circ 2\theta$.

3.4 Scanning Electron Microscopy

SEM images show the silica penetration depth. When increasing the nano-silica content an increase on the penetration depth was observed: ca. $500\ \mu\text{m}$, $630\ \mu\text{m}$ and $740\ \mu\text{m}$ respectively for sample S10-14, S15-14 and S20-14, as shown in Figure 10, 11 and 12. The reactivity of nano-silica with portlandite has been confirmed through SEM images: due to the applied pressure, nano-silica particles are forced into the pores, precipitate on portlandite crystals and react with calcium hydroxide forming additional C-S-

H or C-A-S-H. Unreacted nano-silica was also observed, lying on the surface of cement paste or occluding pores and void space.

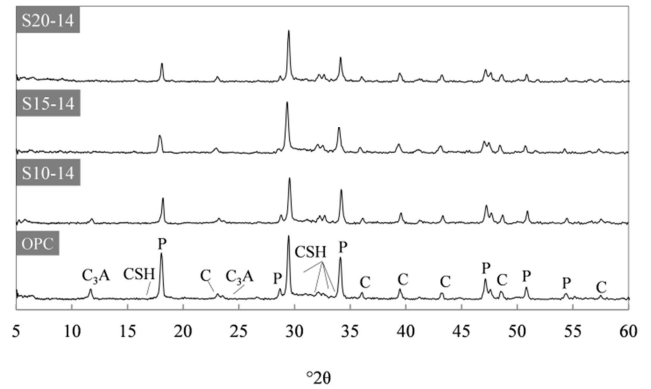


Figure 10. XRD analysis of selected samples. List of the major mineral phases. [P: portlandite; C: calcite; C_3A : calcium aluminate; CSH: calcium silicate hydrates].

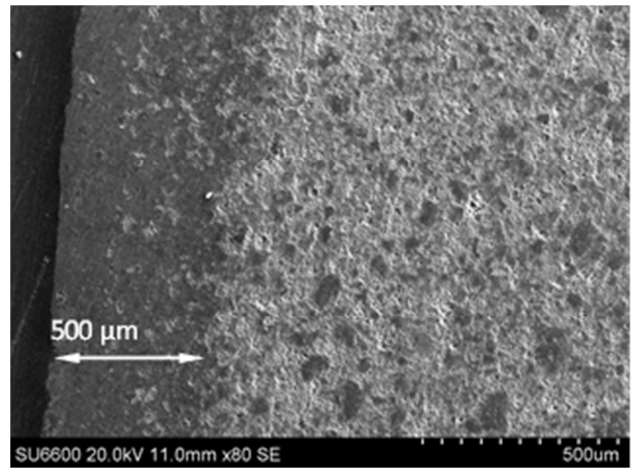


Figure 11. SEM image of sample S10-14.

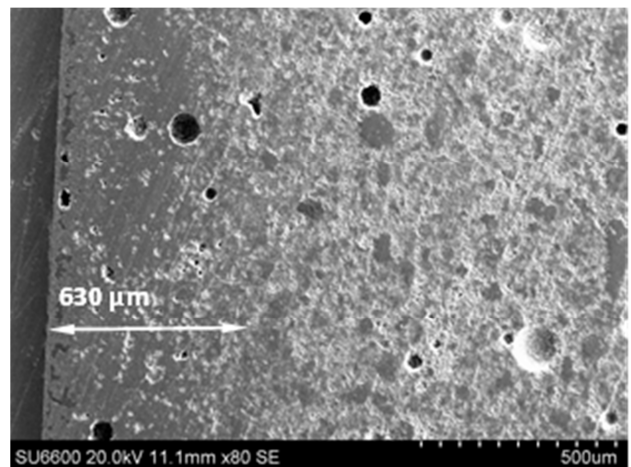


Figure 12. SEM image of sample S15-14.

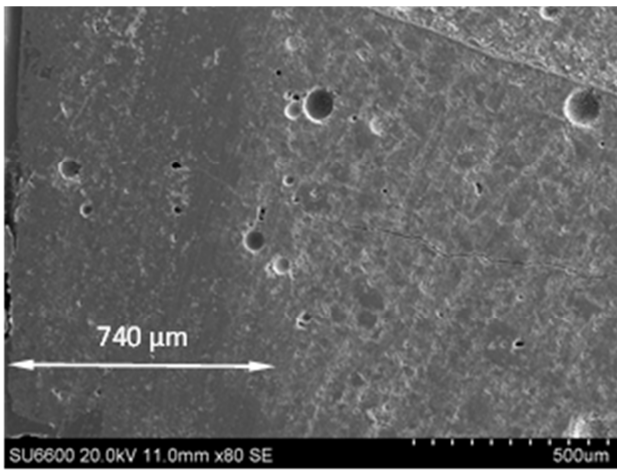


Figure 13. SEM image of sample S20-14.

4 CONCLUSIONS

In this work a novel concrete and cement surface treatment was presented. The following conclusion can be drawn:

1. Low-pressure (20 kPa) silica injection has effectively impregnated cement samples. After 14 days of injection, at the highest nano-silica content (20% wt.) a total reduction of 30% in porosity was observed, suggesting it is a potential consolidant for friable or cracked concrete.
2. Nano-silica injection shows a higher efficiency than silica fume, due to its larger specific surface area and corresponding pozzolanic reactivity.
3. Some of the silica injected has reacted with the calcium hydroxide naturally present in hydrated cement, forming additional binding phases such as C-S-H and C-A-S-H. Unreacted silica however has been absorbed and acts as a filler agent reducing porosity.
4. After 14 days of nano-silica injection an average penetration depth of ca. 745 μm was measured, which is ca. 20% of the cross section of the sample (4 mm).

5 REFERENCES

- Björnström, J. et al., 2004. Accelerating effects of colloidal nano-silica for beneficial calcium-silicate-hydrate formation in cement. *Chemical Physics Letters*, 392(1-3), pp.242–248.
- Cardenas, H.E. & Struble, L.J., 2006. Electrokinetic Nanoparticle Treatment of Hardened Cement Paste for Reduction of Permeability. *Journal of Materials in Civil Engineering*, 18(4), pp.554–560.
- Chen, J.J. et al., 2004. Solubility and structure of calcium silicate hydrate. *Cement and Concrete Research*, 34(9), pp.1499–1519.
- Gallé, C., 2001. Effect of drying on cement-based materials pore structure as identified by mercury intrusion porosimetry. *Cement and Concrete Research*, 31(10), pp.1467–1477.
- Garbev, K. et al., 2008. Cell Dimensions and Composition of Nanocrystalline Calcium Silicate Hydrate Solid Solutions. Part 2: X-Ray and Thermogravimetry Study. *Journal of the American Ceramic Society*, 91(9), pp.3015–3023.
- Hou, P. et al., 2015. Characteristics of surface-treatment of nano-SiO₂ on the transport properties of hardened cement pastes with different water-to-cement ratios. *Cement and Concrete Composites*, 55, pp.26–33.
- Hou, P. et al., 2014. Effects and mechanisms of surface treatment of hardened cement-based materials with colloidal nanoSiO₂ and its precursor. *Construction and Building Materials*, 53, pp.66–73.
- Ji, T., 2005. Preliminary study on the water permeability and microstructure of concrete incorporating nano-SiO₂. *Cement and Concrete Research*, 35(10), pp.1943–1947.
- Jo, B.-W. et al., 2007. Characteristics of cement mortar with nano-SiO₂ particles. *Construction and Building Materials*, 21(6), pp.1351–1355.
- Klimesch, D.S., Ray, A. & Guerbois, J.-P., 2002. Differential scanning calorimetry evaluation of autoclaved cement based building materials made with construction and demolition waste. *Thermochimica Acta*, 389(1-2), pp.195–198.
- Korpa, A. & Trettin, R., 2006. The influence of different drying methods on cement paste microstructures as reflected by gas adsorption: Comparison between freeze-drying (F-drying), D-drying, P-drying and oven-drying methods. *Cement and Concrete Research*, 36(4), pp.634–649.
- Li, H. et al., 2004. Microstructure of cement mortar with nanoparticles. *Composites Part B: Engineering*, 35(2), pp.185–189.
- Pellenq, R.J.-M., Lequeux, N. & van Damme, H., 2008. Engineering the bonding scheme in C-S-H: The iono-covalent framework. *Cement and Concrete Research*, 38(2), pp.159–174.
- Qing, Y. et al., 2007. Influence of nano-SiO₂ addition on properties of hardened cement paste as compared with silica fume. *Construction and Building Materials*, 21(3), pp.539–545.
- Sanchez, F. & Sobolev, K., 2010. Nanotechnology in concrete – A review. *Construction and Building Materials*, 24(11), pp.2060–2071.
- Sánchez, M., Alonso, M.C. & González, R., 2014. Preliminary attempt of hardened mortar sealing by colloidal nanosilica migration. *Construction and Building Materials*, 66, pp.306–312.
- Sha, W., 2002. *Advances in Building Technology*, Elsevier.
- Sha, W., O'Neill, E.A. & Guo, Z., 1999. Differential scanning calorimetry study of ordinary Portland cement. *Cement and Concrete Research*, 29(9), pp.1487–1489.
- Sha, W. & Pereira, G., 2001. Differential scanning calorimetry study of ordinary Portland cement paste containing metakaolin and theoretical approach of metakaolin activity. *Cement and Concrete Composites*, 23(6), pp.455–461.
- Shaw, S., Henderson, C.M. & Komarschek, B., 2000. Dehydration/recrystallization mechanisms, energetics, and kinetics of hydrated calcium silicate minerals: an in situ TGA/DSC and synchrotron radiation SAXS/WAXS study. *Chemical Geology*, 167(1-2), pp.141–159.
- Zhang, J. & Scherer, G.W., 2011. Comparison of methods for arresting hydration of cement. *Cement and Concrete Research*, 41(10), pp.1024–1036.